Impacts of different types of El Niño events on water quality over the Corn Belt, United States

Pan Chen[1,2], Wenhong Li[2,*] and Keqi He[2]

[1] College of Water Resources Science and Engineering, Taiyuan University of Technology, Taiyuan 030024, China
[2] Earth and Climate Sciences, Nicholas School of the Environment, Duke University, NC 27708, USA

Correspondence to: Wenhong Li (wenhong.li@duke.edu)

Abstract. The United States Corn Belt region, which primarily includes two large basins, namely, the Ohio-Tennessee River Basin (OTRB) and the Upper Mississippi River Basin (UMRB), is responsible for the Gulf of Mexico hypoxic zone. Climate patterns such as El Niño can affect the runoff and thus the water quality over the Corn Belt. In this study, the impacts of eastern Pacific (EP) and central Pacific (CP) El Niños on water quality over the Corn Belt region were analyzed using the Soil and Water Assessment Tool (SWAT) models. Our results indicated that at the outlets, annual total nitrogen (TN) and total phosphorus (TP) loads decreased by 13.1% and 14.0% at OTRB, 18.5% and 19.8% at UMRB, respectively, during the EP-El Niño years, whereas during the CP-El Niño years, they increased by 3.3% and 4.6% at OTRB, 5.7% and 4.4% at UMRB, respectively. On the sub-basin scales, more sub-basins showed negative (positive) anomalies of TN and TP during EP- (CP-) El Niño. Seasonal study confirmed that water quality anomalies showed opposite patterns during EP- and CP-El Niño years. At the outlet of OTRB, seasonal anomalies in nutrients matched the El Niño-Southern Oscillation (ENSO) phases, illustrating the importance of climate variables associated with the two types of El Niño on water quality in the region. At the UMRB, TN and TP were also influenced by agriculture activities within the region and their anomalies became greater in the growing seasons during both EP- and CP-El Niño years. Quantitative analysis of precipitation, temperature, and their effects on nutrients suggested that precipitation played a more important role than temperature did in altering water quality in the Corn Belt region during both types of El Niño years. We also found specific watersheds (located in Iowa, Illinois, Minnesota, Wisconsin, and Indiana) that faced the greatest increases in TN and TP loads, were affected by both the precipitation and agricultural activities during the CP-El Niño years. The information generated from this study may help proper decision-making for water environment protection over the Corn Belt.

1 Introduction

The Corn Belt region of the United States (U.S.) primarily includes the Ohio-Tennessee River Basin (OTRB) and the Upper Mississippi River Basin (UMRB) (Kellner and Niyogi, 2015; Panagopoulos et al., 2017; Ting et al., 2021). The Corn Belt is a very important area of the agricultural activity of the country, which is also responsible for the Gulf of Mexico hypoxic zone (Panagopoulos et al., 2014, 2015; Rabalais et al., 2007). The required nutrient reduction of the region to decrease hypoxia is the highest among all regions in the Mississippi River Basin (Mississippi River/Gulf of Mexico Watershed Nutrient Task Force, 2011). Hence, water quality change of the Corn Belt region has been receiving considerable attention.

The El Niño-Southern Oscillation (ENSO) is a coupled ocean-atmosphere phenomenon that occurs across the tropical Pacific (Trenberth, 1997; Wang and Kumar, 2015). Precipitation and temperature are influenced by ENSO in many places in the U.S., including the Corn Belt region (Gershunov, 1998; Lee et al., 2014; Thomson et al., 2003; Wang and Asefa, 2018). For example, more frequent dry conditions were found east of the Ohio River in the early spring of a decaying El Niño (Wang and Asefa, 2018). ENSO events could also have a significant impact on the water quality of a basin through changing climate factors. Heavy or prolonged rains might contribute to the pollutant loading from agricultural runoff (Paul et al., 1997). Temperature anomalies might change river water quality by affecting evaporation and water temperature. Keener et al. (2010) showed that ENSO significantly altered water flow and nitrate concentration in a southeastern U.S. basin. Sharma et al. (2012) found that worse water quality in southeast Alabama was linked to the stream temperature anomalies during El Niño years. However, what are the impacts of ENSO on water quality in the Corn Belt region have not been studied.

In recent years, studies have found two different types of El Niño events: eastern Pacific (EP) and central Pacific (CP) El Niños (Larkin and Harrison, 2005; Li et al., 2011; Tan et al., 2020; Tang et al., 2016; Yeh et al., 2009). The former has warmer sea surface temperature anomalies (SSTAs) in the Niño 3 region (5°N–5°S, 150°W–90°W), while the latter, also called El Niño Modoki, is manifested by maximum SSTAs in the Niño 4 region (5°N–5°S, 160°E–150°W). The effects of these two types of El Niño on regional climate and runoff are different. For example, reduced rainfall was found in the northern, central, and eastern parts of the Amazon during the EP-El Niño years (EP-ENYs), while increased rainfall anomalies were observed in most of the Amazon during the CP-El Niño years (CP-ENYs) (Li et al., 2011). CP-El Niños were more effective in causing drought conditions in India due to atmospheric subsidence than EP-El Niños (Kumar et al., 2006). How these two types of El Niño affect the water quality of the Corn Belt has not been studied. Over recent years, EP-El Niño has appeared less frequently, whereas CP-El Niño has become more common (Kao and Yu, 2009; Yeh et al., 2009). In the future, CP-El Niño will likely happen more frequently (Yeh et al., 2009; Yu et al., 2010). Understanding the impact of these different El Niño events on water quality over the Corn Belt is of critical importance for the water quality management of streams and rivers.

In this study, we used the Soil and Water Assessment Tool (SWAT) model to estimate the water quality changes due to EP- and CP-El Niños over the Corn Belt. The SWAT model is widely used to assess climate change and alternative land use/land management scenarios on runoff and nutrients in a basin (Afonso de Oliveira Serrão et al., 2022; Chaplot et al., 2004; Chen et al., 2021; Johnson et al., 2015; Vaché et al., 2002; Zhang et al., 2020). The

69 detailed objectives of this study were to 1) analyze the impacts of the two types of El Niño on water quality in the

70 Corn Belt region, and 2) identify the main climate factors that affect the change in water quality due to these El

71 Niños. Water quality change associated with future El Niño change was also discussed. Such information is

72 particularly important to enable decision-makers to take timely actions to reduce nutrient loading under climate

73 change.

74 **2 Data and methods**

75 **2.1 Data**

76 The study area includes two large basins in the U.S., namely, OTRB (528,000 km^2) and UMRB (492,000 km^2), as

77 shown in Fig. 1. OTRB comprises a significant portion of Pennsylvania, Ohio, West Virginia, Indiana, Illinois,

78 Kentucky, and Tennessee (Fig. 1a). The amount of annual rainfall in OTRB was high with an average of nearly

79 1200 mm during 1975–2016. OTRB's slopes are steep, especially in the forested Tennessee basin with slopes

80 greater than 5% in most (60%) of the area. The primary land use types are 50% forest, 20% cropland, and 15%

81 pasture (Fig. 1b). The cropland is mainly grown with corn, soybean, and wheat (Santhi et al., 2006). UMRB mainly

82 includes five states: Iowa, Illinois, Missouri, Wisconsin, and Minnesota (Fig. 1a). The mean annual value of rainfall

83 in UMRB during 1975–2016 was 900 mm. UMRB is relatively flat and most of the basin (75%) has a slope lower

84 than 5%. Cropland is the major land use type of the basin (50%) and is primarily grown with corn and soybean (Fig.

85 1b).

86 The weather data were obtained from 2,242 National Weather Service (NWS) stations in the study area. The

87 historical El Niño years were based on Table 1 in Li et al. (2011) and Table 2 in Ren et al. (2018). In summary, nine

88 EP-El Niño events (1976–1977, 1979–1980, 1982–1983, 1986–1987, 1987–1988, 1991–1992, 1997–1998, 2006–

89 2007, and 2015–2016) and six CP-El Niño events (1977–1978, 1990–1991, 1994–1995, 2002–2003, 2004–2005,

90 and 2009–2010) occurred during the study period (1975–2016). Significance was tested by the Monte Carlo method

91 (Levine and Wilks, 2000; Mo, 2010).

92 Available monthly streamflow and water quality data from 1975 to 2016 came from the 15 United States

93 Geological Survey (USGS) gaging stations in the study area. The final data used for calibration and validation of the

94 model were shown in Table 1.

95

96

Hydrology and
Earth System
Sciences
Open Access
Discussions
EGU
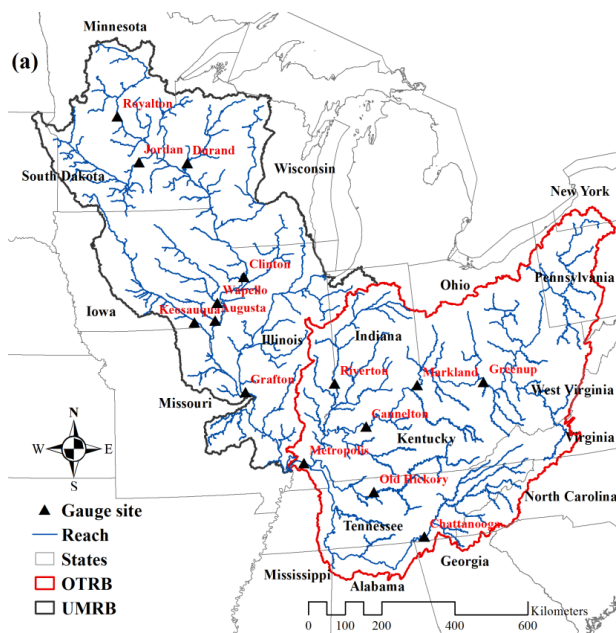
97
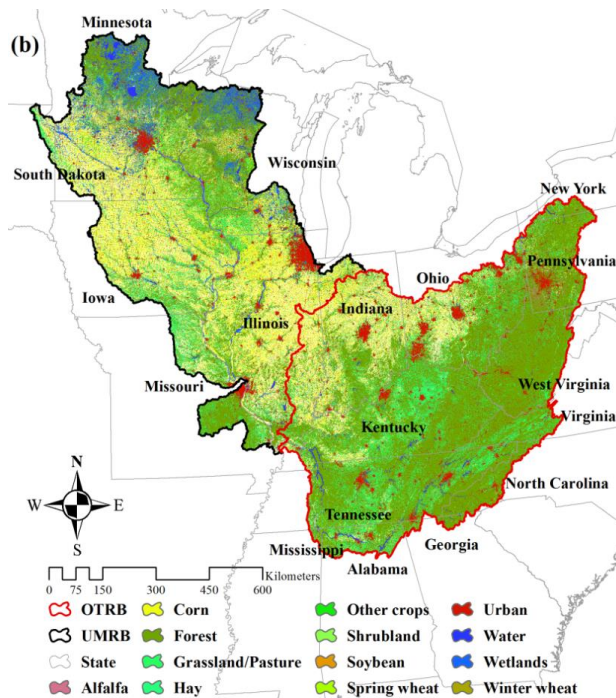
98

99   **Figure 1.** The Ohio-Tennessee River Basin (OTRB) and Upper Mississippi River Basin (UMRB) (a) available
100   United States Geological Survey (USGS) gage sites (black triangles), reaches (light blue), and the two watersheds
101   (heavy red: OTRB, heavy dark: UMRB) and (b) land use/land cover.

Hydrology and
Earth System
Sciences
Open Access
Discussions
EGU

Table 1. Available periods of measured streamflow, total suspended sediment (TSS), total nitrogen (TN), and total phosphorus (TP) at 15 USGS gauge at the OTRB and UMRB

Site Name	Site Number	River Basin	Hydrologically Independent	Drainage (km^2)	Streamflow	TSS	TN	TP
Greenup	03216600		Yes	160,579	1975−2019	-	1975−2019	1975−2019
Markland	03277200		No	215,409	1975−2019	-	-	-
Riverton	03342000		Yes	34,087	1975−2019	-	-	-
Old hickory	03426310	OTRB	Yes	30,233	1988−2007	-	-	-
Cannelton	03303280		No	251,229	1975−2019	-	1975−2019	1975−2019
Metropolis	03611500		No	525,768	1975−2014	-	1975−2016	1975−2016
Chattanooga	03568000		Yes	55,426	1975−2008	-	-	-
Royalton	05267000		Yes	30,044	1975−2019	-	-	-
Jordan	05330000		Yes	41,958	1975−2019	-	-	-
Durand	05369500		Yes	23,336	1975−2019	-	-	-
Clinton	05420500		No	221,703	1975−2019	-	1975−2019	1975−2019
Augusta	05474000	UMRB	Yes	11,168	1975−2019	1975−2017	-	-
Wapello	05465500		Yes	32,375	1975−2019	1978−2017	1978−2019	1977−2019
Keosauqua	05490500		Yes	36,358	1975−2019	-	-	-
Grafton	05587450		No	443,665	1975−2019	1989−2017	1989−2019	1989−2019

2.2 SWAT model description

2.2.1 Model description

SWAT was developed by the U.S. Department of Agriculture Agricultural Research Services (Arnold et al., 1998). It has been widely used in assessing the effects of climate and land use change on hydrological processes, sediment, and nutrients in a basin (Neitsch et al., 2011; Pagliero et al., 2014; Yen et al., 2016). In the SWAT model, a basin is partitioned into sub-basins, which are further divided into hydrological response units (HRUs) (Gassman et al., 2007; Neitsch et al., 2011; Williams et al., 2008). Runoff, sediment, and nutrient loads are simulated for each HRU and then aggregated for the sub-basins (Chen et al., 2021; Gassman et al., 2007; Neitsch et al., 2011). Hence, the pollution situation of each sub-basin during different El Niño years could be obtained from this model.

2.2.2 Model set-up and calibration

In this study, 8-digit Hydrologic Unit Codes (HUC-8) defined by the USGS were selected as SWAT sub-basins. In total, the OTRB and UMRB included 152 and 131 sub-basins, respectively. Flow paths between the sub-basins were determined using the stream network of the National Hydrography Dataset Plus (NHDPlus) dataset developed by the USGS and U.S. Environmental Protection Agency. Each of the sub-basins was further divided into several spatially uniform HRUs based on land use, soil type, and slope (Chen et al., 2021; Neitsch et al., 2011). Thresholds of 0%, 10%, and 5% were used for land use, soil, and slope, respectively, resulting in a total of 20,157 and 20,581 HRUs in the OTRB and UMRB. Then, point sources (Schwarz et al., 2006), crop management (U.S. Department of Agriculture (USDA) - National Agricultural Statistics Service (NASS), 2017), and tillage (Baker, 2011) dataset were incorporated to build the SWAT model (Chen et al., 2021).

SWAT Calibration and Uncertainty Programs (SWAT-CUP) with Sequential Uncertainty Fitting (SUFI-2) algorithm was selected in this large-scale study to complete the calibration of the SWAT model (Abbaspour et al., 2012). The parameters of water flow and water quality in OTRB and UMRB were selected based on a manual experimentation with SWAT parameters and a literature review (Chen et al., 2021; Panagopoulos et al., 2014, 2015; Yen et al., 2016). The calibration steps followed a recent study by Chen et al. (2021). The final parameters were shown in Table S1 and S2 in the supplementary materials. The calibration results indicated that the SWAT model could rationally capture the observation (see Section 2.2.3).

2.2.3 Model performance

Overall, SWAT simulated the water flow of the OTRB and UMRB reasonably well in both calibration (1997–2016) and validation (1975–1996) periods (Table 2). The coefficient of determination (R^2) and Nash-Sutcliffe efficiency (*NSE*) values were larger than 0.5 for almost all the USGS gages except Chattanooga, and percent bias (*PBIAS*) values were all acceptable during the calibration periods (1997–2016) based on the $\leq \pm 25\%$ deviation criterion (Moriasi et al., 2015). The validation results also showed acceptable static values and in some cases were even better, such as Chattanooga and Grafton. Figures

134   S1 and S2 in the supplementary materials further demonstrated good agreement between the calculated and observed

135   streamflow across OTRB and UMRB; particularly, most of the peaks and recession limbs were well matched in the

136   simulations.

137   Modeled water quality was generally in agreement with the observations for the two river basins, as most of the *PBIAS*

138   values were within bias criteria for sediment, TN, and TP during both the calibration and validation periods (Santhi et al.,

139   2014) (Table 3). The only exception that did not meet the criteria was the sediment simulation at Augusta. The upstream

140   drainage area of Augusta was relatively small (only around 3% of the UMRB), thus its influence on downstream sediment

141   and pollutant transport downstream was minor (Fig. 1a). The sediment statistics in OTRB were not calculated here because

142   of a lack of observations (Panagopoulos et al., 2015). Instead, we compared the simulated annual sediment at Metropolis

143   with observations during 1975–2010 and found that the difference was also within the bias criteria for sediment

144   (Panagopoulos et al., 2015; Santhi et al., 2014). Moreover, most of the *NSE* and R^2 values were positive and many R^2 values

145   were greater than 0.5, indicating that the simulated water quality was reasonable (Chen et al., 2021). This finding could be

146   further proved by the graphs of observed and simulated sediment and nutrients (Figs. S3 and S4).

147   **Table 2.** Monthly streamflow calibration and validation statistics.

Gauge Site	Calibration (1997−2016)			Validation (1975−1996)		
	R^2	*NSE*	*PBIAS*	R^2	*NSE*	*PBIAS*
Greenup	0.88	0.87	1.6	0.87	0.82	15.9
Markland	0.88	0.87	6.4	0.88	0.81	17.4
Riverton	0.84	0.83	−1.4	0.8	0.78	−7.4
Old Hickory	0.82	0.75	−4.7	0.81	0.79	7.8
Cannelton	0.89	0.87	9.6	0.9	0.84	15.9
Metropolis	0.84	0.83	4.1	0.88	0.8	15.8
Chattanooga	0.59	0.48	6.1	0.62	0.53	10.7
Royalton	0.63	0.56	−4.7	0.58	0.55	−0.5
Jordan	0.64	0.59	0.7	0.77	0.66	−22.8
Durand	0.65	0.5	−20.9	0.6	0.53	−10.7
Clinton	0.63	0.56	6.6	0.63	0.59	9.8
Augusta	0.75	0.7	−9.9	0.78	0.76	−9.9
Wapello	0.71	0.67	−2.3	0.76	0.76	−1
Keosauqua	0.76	0.73	5.8	0.8	0.78	14
Grafton	0.69	0.62	12.5	0.77	0.7	16.1

148

149

150

151

152

153

Hydrology and
Earth System
Sciences
Open Access
Discussions
EGU

154 **Table 3.** Monthly TSS, TN, and TP calibration and validation statistics.

Variable	Gauge Site	Calibration(1997−2016)			Validation(1975−1996)		
		R^2	NSE	PBIAS	R^2	NSE	PBIAS
TSS	Augusta	0.34	0.1	64.5	0.39	0.02	77.2
	Wapello	0.45	0.15	−21.5	0.51	0.48	13.6
	Grafton	0.43	0.22	0.7	0.26	0.07	13.9
TN	Greenup	0.57	0.23	−13.7	0.59	0.52	17
	Cannelton	0.63	0.59	8.3	0.59	0.46	26.9
	Metropolis	0.58	0.36	−9.2	0.57	0.51	14.9
	Clinton	0.43	−0.61	2.7	0.36	−0.25	9.4
	Wapello	0.51	0.05	1.8	0.44	0.32	17.6
	Grafton	0.54	0.15	2.2	0.53	0.08	2
TP	Greenup	0.56	0.46	−29.6	0.59	0.57	8.6
	Cannelton	0.56	0.48	21.2	0.44	0.35	28.1
	Metropolis	0.49	0.41	−8.6	0.45	0.38	−5.2
	Clinton	0.44	−0.59	−11.1	0.42	0.13	10.9
	Wapello	0.6	0.24	−19.1	0.55	0.29	−16.3
	Grafton	0.57	0.25	0.8	0.54	0.12	−14.8

155 **3 Results**

156 **3.1 Impacts of the EP- and CP-El Niños on the water quality in the Corn Belt**

157 **3.1.1 Annual composite**

158 (1) Water quality at the outlet

159 Table 4 lists the nutrient change during EP- and CP-ENYs at the outlet of OTRB and UMRB. Annual loads of TN and TP

160 decreased during the EP-ENYs, while the pattern reversed during the CP-ENYs in the U.S. Corn Belt region. Specifically,

161 compared to normal years, the TN and TP decreased by 13.1% (61,300 metric ton yr^{-1}, hereafter ton yr^{-1}) and 14.0% (7,300

162 ton yr^{-1}) during EP-ENYs, respectively, whereas they increased by 3.3% (15,500 ton yr^{-1}) and 4.6% (2,400 ton yr^{-1}) during

163 CP-ENYs at the outlet of the OTRB, respectively (Table 4). TN and TP at the outlet of the UMRB showed a similar pattern

164 as that of the OTRB, decreasing (increasing) by 18.5% (5.7%) and 19.8% (4.4%) in EP (CP)-ENYs. Furthermore, EP-El

165 Niños had a much greater impact on water quality than CP-El Niños at the outlets of OTRB and UMRB. The magnitudes of

166 variation in both TN and TP during the EP-ENYs were three to four times greater than those during the CP-ENYs (Table 4).

167

168

169

Hydrology and
Earth System
Sciences
Discussions

Table 4. Soil and Water Assessment Tool (SWAT) model's estimates of annual mean TN and TP at the outlets of the OTRB and UMRB during all simulation year (1975−2016), eastern Pacific (EP)-El Niño years and central Pacific (CP)-El Niño years.

River Basin	Variable	Average	EP		CP	
			Anomaly	Percent (%)	Anomaly	Percent (%)
OTRB	TN ($\times 10^3$ ton yr^{-1})	469.0	−61.3	−13.1	15.5	3.3
	TP ($\times 10^3$ ton yr^{-1})	52.2	−7.3	−14.0	2.4	4.6
UMRB	TN ($\times 10^3$ ton yr^{-1})	526.2	−97.5	−18.5	29.9	5.7
	TP ($\times 10^3$ ton yr^{-1})	41.0	−8.1	−19.8	1.8	4.4

(2) Water quality at the sub-basin scale

We analyzed water quality change on the sub-basin scale during EP-ENYs and CP-ENYs, respectively (Fig. 2). Anomalous patterns of water quality associated with El Niño events within the Corn Belt varied in space. Clearly, more sub-basins showed negative anomalies of TN and TP during EP-ENYs, whereas more sub-basins showed positive anomalies during CP-ENYs (Fig. 2). Specifically, during EP-ENYs, significant below-average TN and TP were found almost in the whole OTRB and UMRB with maximum reductions of TN and TP up to −11.7 and −0.9 kg ha^{-1}, respectively, which were of similar magnitudes to the mean values (12.7 kg of N ha^{-1} and 1.0 kg of P ha^{-1}) in the Corn Belt region (Figs. 2a and 2b). During CP-ENYs, positive anomalies mainly occurred throughout the southern OTRB and UMRB. In the northern UMRB and OTRB, about 42.4% and 41.7% of sub-basins tended to have below-average TN and TP (Figs. 2c and 2d). These patterns coincided with the TN and TP changes at the outlets of the two basins, which could also explain why greater changes in TN and TP occurred in EP-ENYs than in CP-ENYs at the outlets of the OTRB and UMRB (Table 4).

186
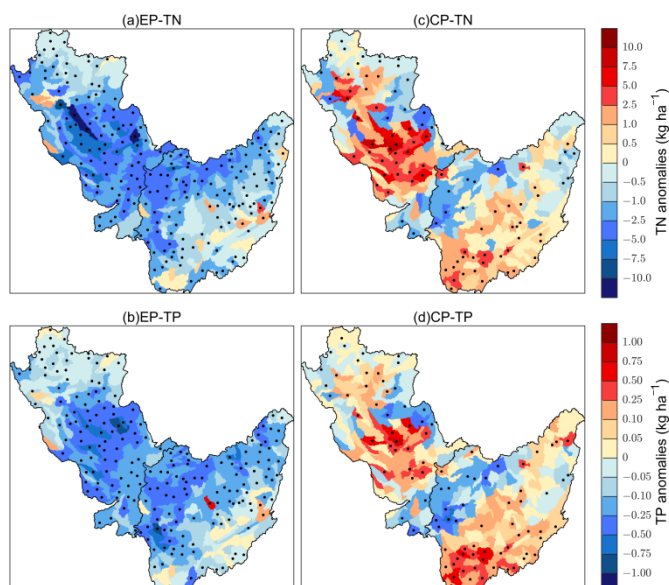
Figure 2. Composite results of annual TN and TP anomalies (unit: kg ha^{-1}) in EP-El Niño years (a and b) and in CP-El Niño

years (c and d) during the period of 1975–2016. Stippling denotes anomalies significantly different from zero at the 95%

confidence level based on the Monte Carlo test.

190

3.1.2 Seasonal composite

(1) Water quality at the outlet

Figure 3a showed TN anomalies at the OTRB and UMRB outlets in each season during EP- and CP-ENYs. At the outlet of

the OTRB, Seasonal anomalies of the water quality reached the maximum when ENSO signals were the strongest (Fig. 3a).

El Niño usually developed in boreal summer (June-August, JJA) and autumn (September-November, SON), peaked in

winter (December of the current year and January and February of the following year, DJF), and decayed in spring (March-

May, MAM) (Trenberth, 1997; Li et al., 2011). Maximum changes in TN occurred in the winter and spring seasons during

EP-ENYs (decreased by 28.3×10^3 and 29.5×10^3 metric tons (hereafter ton), respectively, Fig. 3a). During CP-ENYs, TN

increased by 11.7×10^3 tons in winter, and did not change much in the rest of the three seasons (spring, summer, and autumn)

compared to that in the normal years (Fig. 3a). Seasonal TN anomalies at the outlet of the UMRB were different from those

of the OTRB. Figure 3a showed that TN decreased by 71.0×10^3 and 30.8×10^3 tons, respectively, in the spring and summer

seasons during EP-ENYs; but in winter and autumn, TN did not change much compared to normal years. Similarly, during

CP-ENYs, TN anomalies were greater in spring and summer although TN anomalies became positive during CP-ENYs,

different from TN changes during EP-ENYs (Fig. 3a).

205   Figure 3b demonstrated that the seasonal changes of TP during EP- and CP-ENYs were similar to those of TN in both

206   OTRB and UMRB during EP-ENYs. At the OTRB the magnitudes of TP reduction in boreal winter and spring were greater

207   than those in the summer and autumn seasons during EP-ENYs. During CP-ENYs, TP anomalies were greater in both

208   autumn and winter (Fig. 3b). This phenomenon was probably related to the different duration of the two types of El Niño.

209   The mean duration of EP-El Niño was about 15 months (Mo, 2010), its impact on water quality could last into the following

210   spring; while El Niño Modoki usually lasted for about eight months (Mo, 2010, Yu et al., 2010), therefore the impacts of the

211   CP-El Niño on water quality usually ended in the winter. Besides, at the UMRB maximum changes in TP occurred in the

212   spring and summer seasons during both EP- and CP-ENYs.

213   In summary, more seasons showed negative anomalies of water quality during EP-ENYs, whereas more seasons showed

214   positive anomalies during CP-ENYs (Fig. 3). Consequently, the annual TN and TP anomalies over the Corn Belt region

215   showed the opposite pattern during EP-ENYs and CP-ENYs (Table 4).

216

217
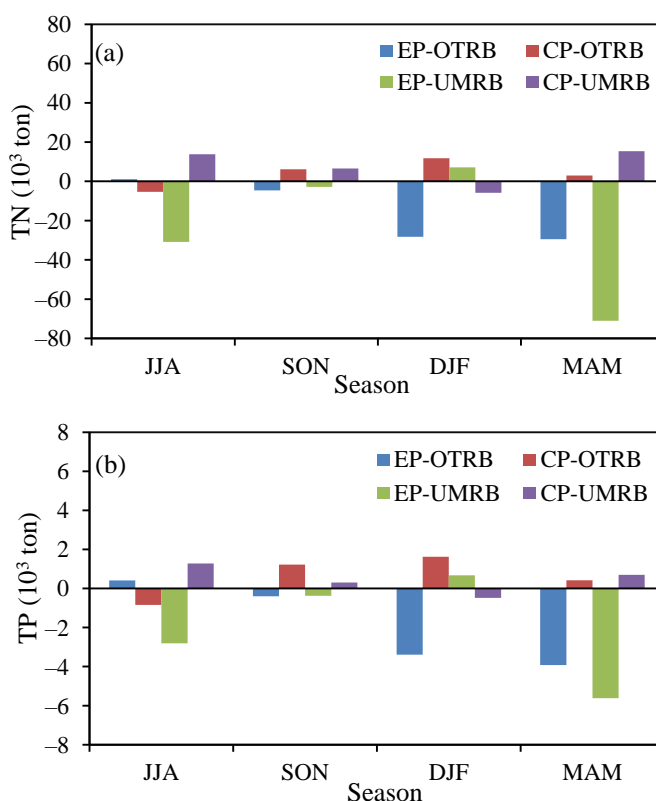
Figure 3. Seasonal anomalies of (a) TN and (b) TP (unit: 10^3 tons) in summer (June-August, JJA), autumn (September-November, SON), winter (December of the current year and January and February of the following year, DJF) and spring (March-May, MAM) at the outlets of the OTRB and UMRB during EP-El Niño years and CP-El Niño years.

221

222

11

Hydrology and
Earth System
Sciences
Open Access
EGU
Discussions

223   (2) Water quality at the sub-basin scale

224   Water quality at the Corn Belt can vary in different locations/sub-basins and change between seasons. Figure 4 showed

225   spatial patterns of TN and TP anomalies at the OTRB and UMRB in each season during the CP- and EP-ENYs, separately.

226   EP-El Niño was characterized by negative TN and TP anomalies over most of the OTRB and UMRB for all seasons (Figs.

227   4a–4d and 4i–4l). Significant below-average TN and TP occurred in almost all of the UMRB and the eastern OTRB in the

228   summer when EP-El Niño was developing in the tropical Pacific, with maximum reductions up to −4.5 and −0.45 kg ha^{-1},

229   respectively (Figs. 4a and 4i). The negative water quality anomalies moved to the southern UMRB and northern OTRB in

230   the autumn (Figs. 4b and 4j). These negative anomalies further moved to the whole OTRB when EP-El Niño was mature in

231   the winter (Figs. 4c and 4k). This result generally agreed with previous findings of the El Niño impacts on the precipitation

232   in the study area, which indicated that the precipitation in the Ohio Valley was sensitive to El Niño events and showed

233   negative precipitation anomalies at EP-ENYs (Mo, 2010; Twine et al., 2005). In spring, severe TN and TP deficits were most

234   apparent almost all over the Corn Belt area (Figs. 4d and 4l).
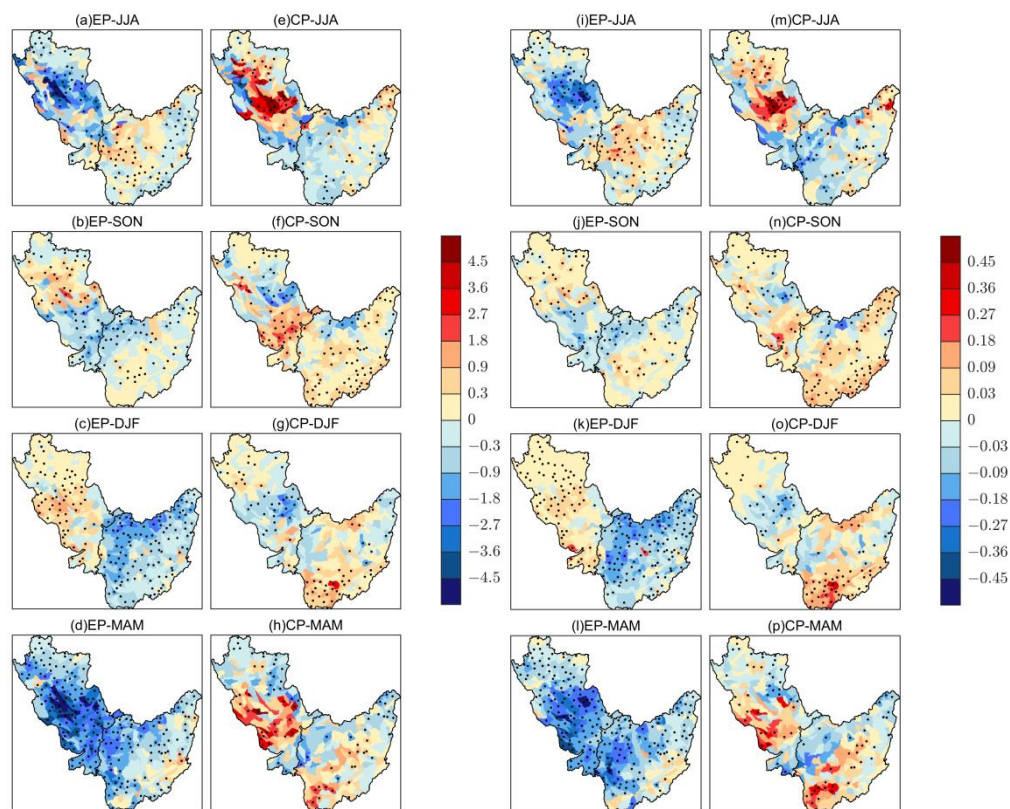
235

236   **Figure 4.** Seasonal composite of (a-h) TN and (i-p) TP anomalies (unit: kg ha^{-1}) in summer (JJA) (a and i), autumn (SON)

237   (b and j), winter (DJF) (c and k), and spring (MAM) (d and l) in EP-El Niño years during the period of 1975–2016; (e-h) and

238   (m-p) are the same as (a-d) and (i-l) but for CP-El Niño years. Stippling denotes anomalies significantly different from zero

239   at the 95% confidence level based on the Monte Carlo test.

Hydrology and
Earth System
Sciences
Open Access
Discussions
EGU

240　In contrast, during CP-ENYs, positive TN and TP anomalies were scattered in most of the Corn Belt region with the

241　highest TN and TP anomalies increase up to 4.5 and 0.45 kg ha^{-1}, respectively (Figs. 4e–4h and 4m–4p). In summer,

242　northern UMRB and eastern OTRB were characterized by above-normal water quality (Figs. 4e and 4m). The positive TN

243　and TP anomalies moved to the southern UMRB and whole OTRB in the autumn (Figs. 4f and 4n). In winter, these positive

244　anomalies were concentrated in the southern OTRB and northern UMRB (Figs. 4g and 4o). In the spring, abnormally high

245　TN and TP mainly occurred in the southern part of the UMRB while most of the positive and negative anomalies in the

246　OTRB region were insignificant (Figs. 4h and 4p).

247　　In conclusion, water quality anomalies showed opposite patterns during EP-ENYs and CP-ENYs on both annual and

248　seasonal time scales in the Corn Belt region. Furthermore, EP-El Niño seemed to have a greater and long-lasting impact on

249　TN and TP than CP-El Niño. Hence, treating the two as a single phenomenon was not appropriate when analyzing the

250　impacts of ENSO on water quality.

251　**3.2 Possible climate reasons for the water quality change during CP- and EP-El Niño events**

252　As precipitation and temperature usually respond differently to the two types of El Niño at different temporal and spatial

253　scales (Li et al., 2011; Tan et al., 2020), we hereafter analyzed these climate factors' impacts accordingly in the Corn Belt

254　region.

255　**3.2.1 Precipitation**

256　Decreased precipitation in EP-ENYs was one of the important reasons that improved water quality in the Corn Belt region.

257　This finding could be shown in the spatial patterns of annual precipitation (Fig. 5a), and TN and TP anomalies (Figs. 2a and

258　2b). For example, significantly below-normal precipitation occurred in much of the OTRB and UMRB (278 out of 283 sub-

259　basins) during EP-ENYs (Fig. 5a), thus TN and TP were reduced in most parts of the Corn Belt (Figs. 2a and 2b). During

260　CP-ENYs, precipitation anomalies became positive in 226 out of 283 sub-basins (Fig. 5c). Correspondingly, TN and TP

261　concentrations were elevated compared to normal years (Figs. 2c and 2d). Spatially, there were more sub-basins (98.2%) and

262　larger area with negative precipitation anomalies in EP-ENYs than positive anomalies (79.9% sub-basins) during CP-ENYs

263　in the Corn Belt, indicating that EP-El Niño tended to have a much wider impact on precipitation and thus water quality than

264　CP-El Niño.

265　　To better understand how precipitation affected water quality in the Corn Belt, variations of annual runoff during EP-

266　ENYs and CP-ENYs were also discussed because nitrogen and phosphorus were transported by runoff (Neitsch et al., 2011),

267　and precipitation was a very important source of runoff (Gassman et al., 2007). The overall patterns of runoff anomalies

268　(Figs. 5b and 5d) were similar to those of precipitation anomalies (Figs. 5a and 5c) during the two types of El Niño with

269　pattern correlations being 0.79 at OTRB and 0.75 at UMRB in EP-ENYs, 0.96 and 0.77 in CP-ENYs, respectively.

270　Specifically, during EP-ENYs, negative annual runoff anomalies occurred in most of the Corn Belt region (Fig. 5b),

271　resulting in reduced TN and TP compared to normal years (Figs. 2a and 2b). In contrast, in CP-ENYs, positive runoff

272   anomalies were mainly concentrated in southern OTRB and UMRB (Fig. 5d), more nutrients were thus carried out by the

273   runoff associated with above-normal precipitation in the area (Figs. 2c and 2d). We also noticed that EP-El Niño had a wider

274   influence on runoff than CP-El Niño, as 71 more sub-basins (259 vs 188) and larger areas with significant runoff anomalies

275   were found in EP-ENYs than in CP-ENYs (Figs. 5b and 5d), generally consistent with the spatial patterns of precipitation

276   changes due to the El Niños (Figs. 5a and 5c). The phenomena could partly explain why EP-El Niños tended to have greater

277   impacts on the water quality than CP-El Niños at the outlets of the OTRB and UMRB.

278   Some differences also existed among precipitation, runoff, and nutrients. For precipitation and runoff, annual precipitation

279   anomalies were greater than runoff anomalies in the El Niño years. For example, precipitation anomalies of many sub-basins

280   in northern UMRB were stronger than -0.2 mm day^{-1} during EP-ENYs, but the magnitudes of runoff anomalies were

281   weaker than -0.2 mm day^{-1} (Figs. 5a and 5b). During CP-ENYs, most annual precipitation and runoff anomalies were

282   positive, but the magnitudes of precipitation anomalies were generally higher than that of runoff anomalies (Figs. 5c and 5d).

283   These findings suggested that the impact of El Niño on runoff was weakened by the land surface hydrological process. For

284   runoff and nutrients, changes of runoff in El Niño years were greater in the OTRB than in the UMRB (Figs. 5b and 5d),

285   whereas changes of TN and TP were smaller in the OTRB than in the UMRB during both EP-ENYs and CP-ENYs (Fig. 2).

286   The discrepancies between annual runoff and nutrient anomalies in the OTRB and UMRB may be related to the presence of

287   more cropland in the UMRB where more fertilizers were used (Chen et al., 2021, see Section 4.1 for details), hence a

288   relatively small change of runoff due to El Niño-induced precipitation could lead to large TN and TP variations.
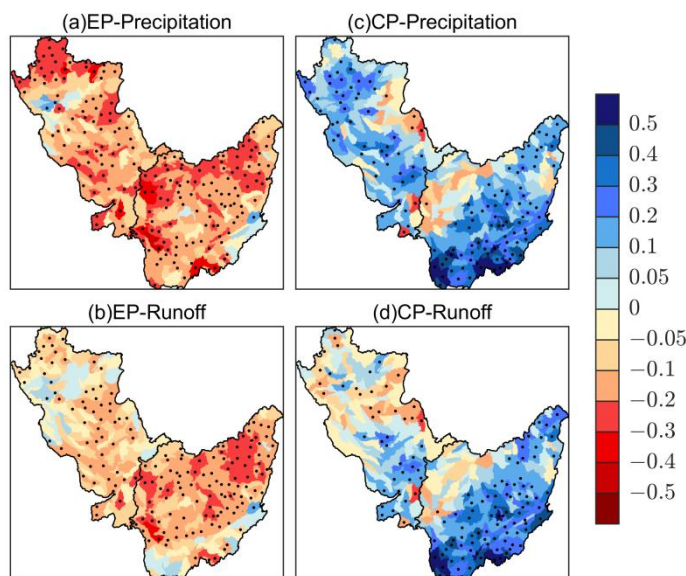

289

290   **Figure 5.** Composite of annual precipitation and runoff anomalies (unit: mm day^{-1}) for the two types of El Niño during the

291   period of 1975–2016 (a and b) in EP-El Niño years and (c and d) in CP-El Niño years. Stippling denotes anomalies

292   significantly different from zero at the 95% confidence level based on the Monte Carlo test.

293   Seasonal patterns of precipitation and runoff anomalies (Fig. 6) further proved the impacts of precipitation on water

294   quality through runoff during EP-ENYs and CP-ENYs. In summer, significantly below-normal precipitation occurred in

295   almost all of the UMRB when EP-El Niño was developing in the tropical Pacific, with maximum reductions of precipitation

296   up to -0.9 mm day^{-1} in the region (Fig. 6a). The runoff anomaly pattern was much the same as that of precipitation, but in a

297   weaker magnitude—less than -0.6 mm day^{-1} in UMRB (Fig. 6i). At the same time, TN and TP decreased in the area (Figs.

298   4a and 4i) because fewer nutrients were carried out by the reduced runoff in summer (Fig. 6i). Similar change patterns of

299   precipitation (Figs. 6b-6d), runoff (Figs. 6j-6l), and nutrients (Figs. 4b-4d and 4j-4l) could also be found in other seasons

300   during EP-ENYs. We noticed that negative runoff and precipitation anomalies reached their maximum in spring throughout

301   the Corn Belt, leading to better water quality in the region compared to the normal years. CP-El Niño events caused the

302   opposite patterns of seasonal precipitation (Figs. 6e-6h) and runoff anomalies (Figs. 6m-6p) in the Corn Belt region; TN and

303   TP thus increased in central and southern UMRB in the spring, summer, and autumn, and most of OTRB from autumn to

304   winter (Figs. 4e-4h and 4m-4p). Some differences also existed between precipitation and water quality in the UMRB,

305   especially in spring and summer. During these two seasons, the variation of the seasonal precipitation at each sub-basin was

306   relatively uniform in both EP-ENYs (Figs. 6a and 6d) and CP-ENYs (Figs. 6e and 6h), but nutrient variations were high in

307   some sub-basins of the UMRB (Figs. 4a, 4d, 4e, 4h, 4i, 4l, 4m, and 4p). This phenomenon suggested that water quality was

308   also influenced by local factors besides climate variables associated with El Niños.

309

Hydrology and
Earth System
Sciences
Discussions
Open Access
EGU
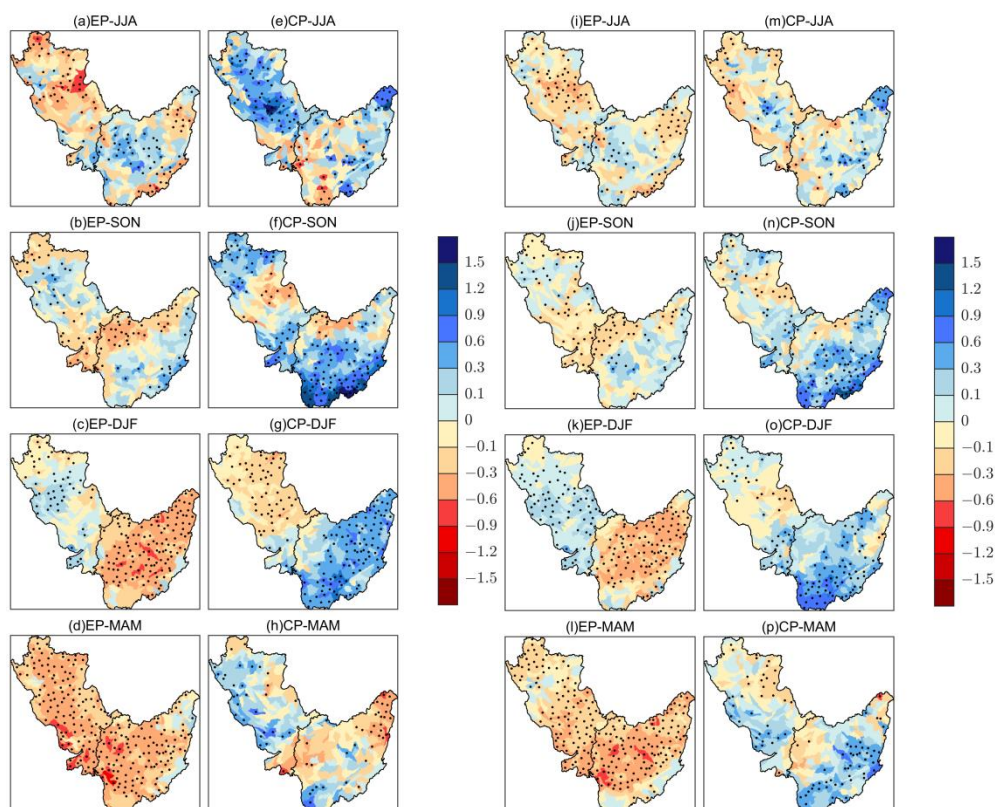
Figure 6. Composite of seasonal (a-h) precipitation and (i-p) runoff anomalies (unit: mm day^{-1}) in JJA (a and i), SON (b and j), DJF (c and k), and MAM (d and l) in EP-El Niño years during the period of 1975−2016; (e-h) and (m-p) are the same as (a-d) and (i-l) but for CP-El Niño years. Stippling denotes anomalies significantly different from zero at the 95% confidence level based on the Monte Carlo test.
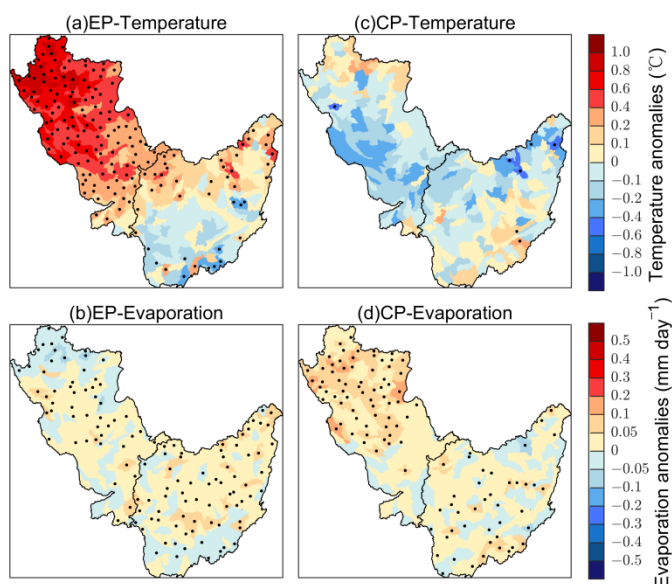
3.2.2 Temperature

Temperature changes have previously been found to affect water quality by changing the evaporation process of the water cycle (Neitsch et al., 2011 Sun et al., 2011). Thus, how evaporation varied associated with temperature change during El Niños in the Corn-Belt region was analyzed. Compared to normal years, the annual temperature increased over the UMRB, but decreased in the OTRB, especially in the southern OTRB during EP-ENYs (Fig. 7a). Evaporation slightly increased in most of OTRB (Fig. 7b), which did not share the same pattern with temperature change on the annual time scale (Fig. 7a). This might be due to the fact that temperature directly affected potential evapotranspiration (Neitsch et al., 2011), the ability of the atmosphere to remove water from the surface through both evaporation and transpiration, but the actual evaporation/evapotranspiration was also related to other variables such as the amount of water available for evaporation besides temperature. Enhanced evaporation further reduced runoff (Bales et al., 2017). Thus, decreased precipitation (Fig. 5a)

326 and enhanced evaporation (Fig. 7b) during the EP-ENYs would facilitate runoff decline and cause a much wider impact of

327 EP-El Niño events on water quality in the Corn Belt region (Fig. 2). During CP-ENYs, temperature decreased insignificantly

328 in most of the Corn Belt region (Fig. 7c). Evaporation increased in more sub-basins over the UMRB (Fig. 7d). The enhanced

329 evaporation (Fig. 7d) tended to offset, to some extent, the impact of higher than normal precipitation (Fig. 5c) on water

330 quality during CP-ENYs.

331   The impacts of the two climate factors, precipitation and temperature (through evaporation), on runoff were compared.

332 During the El Niño years, the magnitude of annual precipitation change was often greater than 0.1 mm day^{-1} (Figs. 5a and 5c)

333 while most of the annual evaporation varied between -0.05 and 0.05 mm day^{-1} (Figs. 7b and 7d). This suggested that both

334 precipitation and evaporation influence water quality through runoff, but precipitation seemed to play a more important role

335 in altering water quality over the Corn Belt region during El Niño years.


336

337 **Figure 7.** Composite results of annual average temperature (a and c, unit: °C) and evaporation (b and d, unit: mm day^{-1})

338 anomalies for EP-El Niño years (a and b) and CP-El Niño years (c and d), respectively. Stippling denotes anomalies

339 significantly different from zero at the 95% confidence level based on the Monte Carlo test.

340

341   Figure 8 showed seasonal patterns of temperature and evaporation anomalies during the CP- and EP-ENYs. In EP-ENYs,

342 significantly below-normal temperature occurred throughout the OTRB in the summer (Fig. 8a) and expanded to the entire

343 Corn Belt region in the autumn (Fig. 8b). In winter and spring, significantly positive temperature anomalies were shown in

344 the UMRB and most of OTRB (Figs. 8c and 8d). Corresponding to the seasonal temperature anomalies, evaporation varied

345 differently at different seasons (Figs. 8i-8l). In the summer and autumn, most sub-basins had negative evaporation anomalies

346 with decreased temperature (Figs. 8i and 8j); but in winter and spring, significantly above-normal evaporation occurred with

347 increased temperature in EP-ENYs (Figs. 8k and 8l). During CP-ENYs, the summer season was characterized by negative

Hydrology and
Earth System
Sciences
Discussions

Open Access

EGU

348   temperature anomalies throughout the Corn Belt region, with the maximum anomalies up to −1.2 ℃ (Fig. 8e). Evaporation

349   anomalies became negative in most sub-basins (Fig. 8m). The temperature pattern was reversed in the autumn, with positive

350   temperature and evaporation anomalies over the entire region (Figs. 8f and 8n). In winter, temperature anomalies became

351   negative again (Fig. 8g), evaporation also reduced, with significantly negative anomalies in the OTRB and central and

352   southern UMRB (Fig. 8o). Temperature anomalies in spring were insignificant (Fig. 8h) most likely due to the short eight-

353   month duration of the CP-El Niño (Mo, 2010, Yu et al., 2010), although positive evaporation anomalies appeared in the

354   northern UMRB (Fig. 8p).
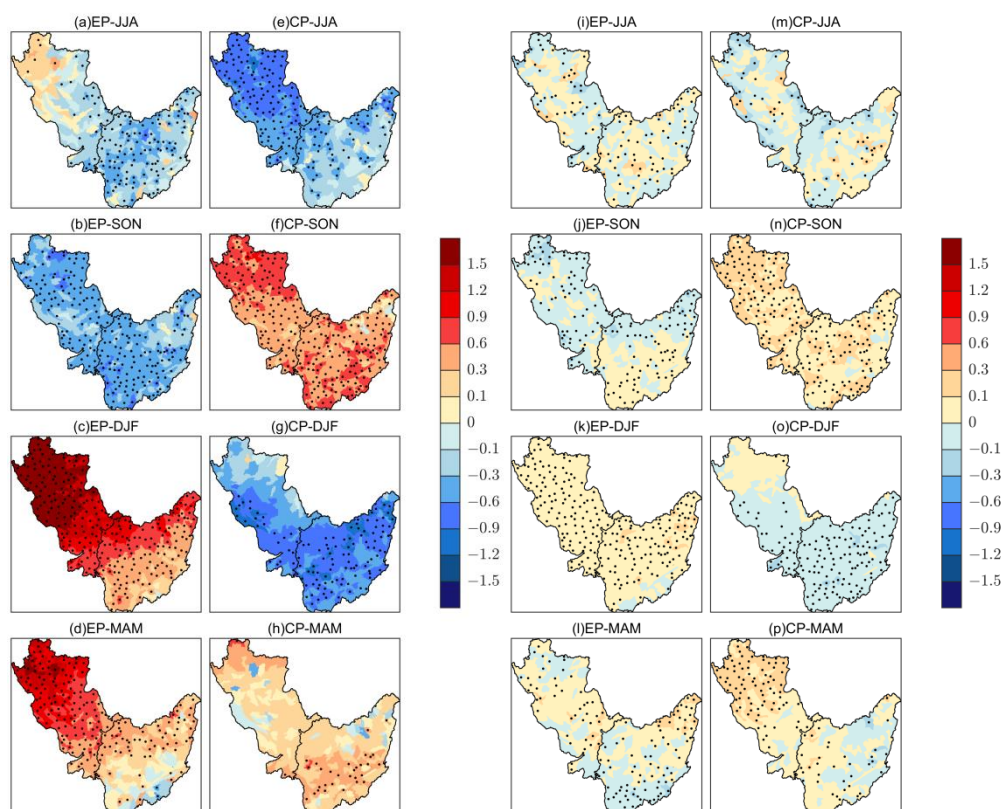
355

356   **Figure 8.** Composite results of seasonal temperature (a-h, unit: °C) and evaporation (i-p, unit: mm day^{-1}) anomalies in JJA (a

357   and i), SON (b and j), DJF (c and k), and MAM (d and l) in EP-El Niño years (a-d, i-l) and CP-El Niño years (e-h, m-p),

358   respectively. Stippling denotes anomalies significantly different from zero at the 95% confidence level based on the Monte

359   Carlo test.

360

361 **4 Discussion**

362 **4.1 Agricultural activity**

363 This study focused on climate impact on water quality during EP-ENY and CP-ENY, we did not perform sensitivity

364 experiments on agriculture activities. In the SWAT model runs, the distribution of agriculture activities pattern (2008

365 Cropland Data Layers (CDL); USDA-NASS, 2016) was kept the same during El Niño and normal years. Corresponding to

366 the described agriculture activities, the corn growing areas, i.e., the southern UMRB and northern OTRB, usually produced

367 greater annual TN loads (>10 kg of N ha^{-1}) and TP loads (>1 kg of P ha^{-1}) (Fig. S5). During EP-ENYs, the nutrients were

368 largely reduced (>1 kg of N ha^{-1} and >0.1 kg of P ha^{-1}) in the two corn-growing regions because of decreased precipitation

369 (< -0.1 mm day^{-1}) (Figs. 2a, 2b, and 5a). In CP-ENYs, the nutrient level increased in the southern UMRB (Figs. 2c and 2d)

370 since enhanced precipitation in CP-ENYs exacerbated the water quality in the area of heavy agriculture activities (Fig. 5c).

371 Water quality in the OTRB region showed different change patterns from the agriculture activities, i.e., TN and TP decreased

372 in the northern OTRB but increased in the southern OTRB (Figs. 2c and 2d). Such changes in water quality followed the

373 precipitation change in the OTRB (Fig. 5c), demonstrating that CP-El Niño-induced precipitation change played a more

374 important role in modulating water quality in OTRB.

375 On seasonal scales, changes in nutrients' magnitudes were stronger in spring and summer, especially in UMRB (Fig. 4).

376 This pattern was also related to the growth period of crops in the Corn Belt. The major crops here are corn and soybean,

377 which are often planted and fertilized in May and harvested in October. Hence, nutrients might be more likely to be removed

378 from the soil during spring and summer.

379 **4.2 Equivalent impacts of CP- and EP-El Niño on water quality in specific watersheds**

380 Section 3 discussed the impacts of El Niño on water quality at the outlets and sub-basin scales. At the outlets, EP-El Niño

381 had a much greater impact on TN and TP than CP-El Niño both at annual and seasonal time scales. But at the sub-basin scale,

382 CP- and EP-El Niño could have equivalent impacts on water quality in specific watersheds, predominantly in Iowa (IA),

383 Illinois (IL), Minnesota (MN), Wisconsin (WI), and Indiana (IN), which contributed the greatest amounts of nutrient change

384 to the whole basin loads (Fig. 2). Table 5 listed the top 10 HUC-8 sub-basins with the largest nutrient change during the two

385 types of El Niño years. In EP-ENYs, TN anomalies changed from 6.2 and 11.7 kg ha^{-1} among the top 10 HUC-8 sub-basins;

386 while in CP-ENYs, TN anomalies changed from 5.6 and 9.3 kg ha^{-1} (Table 5). These changes in TN during classic El Niño

387 and El Niño Modoki were comparable. Analysis of the top 10 HUC-8 sub-basins with the largest TP change during the EP-

388 and CP-El Niño illustrated similar results (not shown). These findings indicated that CP-El Niño could have comparable

389 impacts on TN and TP as EP-El Niño at the hot spot sub-basins although EP-El Niño had a much broader and longer impact

390 on water quality at the outlets.

391

392 **Table 5.** Information on the top 10 8-digit Hydrologic Unit Codes (HUC-8) sub-basins with greatest TN anomalies during

393 EP- and CP-El Niño years.

El Niño Type	HUC-8	TN (kg ha^{-1})		Precipitation (mm yr^{-1})		Cropland Percentage (%)	States
		Average	Anomaly	Average	Anomaly		
EP	07080102	51.2	−11.7	912.9	−54.8	70.1	IA,MN
	07080201	33.7	−10.8	909.9	−51.1	73.5	IA,MN
	07090006	37.8	−10.4	935.2	−65.7	68.8	IL,WI
	07020011	28.3	−8.5	845.1	−84.0	78.6	MN
	07080202	27.4	−7.5	890.2	−32.9	72.1	IA,MN
	05120107	24.8	−7.2	1068.8	−102.2	73.8	IN
	07090007	31.2	−6.9	949.4	−87.6	78.9	IL
	07080204	33.0	−6.6	918.0	−69.4	76.0	IA
	07080208	27.0	−6.3	904.4	−62.1	59.9	IA
	07080209	25.6	−6.2	914.8	−94.9	58.4	IA
CP	07080103	26.2	9.3	948.0	142	70.2	IA
	07080208	27.0	9.1	904.4	135	59.9	IA
	07080206	21.9	9.1	923.1	128	63.3	IA
	07090007	31.2	7.3	949.4	62	78.9	IL
	07080203	24.2	6.8	855.4	124	68.1	IA,MN
	07080102	51.2	6.5	912.9	51	70.1	IA,MN
	07020007	16.5	6.1	778.0	69	73.2	MN
	07090006	37.8	5.9	935.2	18	68.8	IL,WI
	07060006	24.4	5.6	911.8	44	59.3	IA
	07130009	20.6	5.6	1005.0	124	80.9	IL

394

4.3 Future water quality change

396 Existing studies suggested that CP-El Niño episodes occurred more frequently in a warming climate (Yeh et al., 2009; Yu et

397 al., 2010). We found that annual loads of TN and TP tend to increase in the Corn Belt region during CP-ENYs in the current

398 climate. As CP-El Niño frequency increases in the future, TN and TP loads would likely increase over the Corn Belt region

399 even under the same agricultural conditions, indicating a possible deterioration of water quality in this region when the

400 climate warms.

401 The spatial patterns of TN and TP anomalies during CP-ENYs (Fig. S6) also suggested that specific watersheds,

402 predominantly in southern UMRB and western OTRB, such as Iowa, Illinois, Wisconsin, Indiana, and Kentucky, will likely

Hydrology and
Earth System
Sciences
Discussions
EGU
Open Access

403 experience the most increases of TN and TP loads in the future. Such information is critical to ensure proper decision-
404 making for watershed protection.

4.4 Limitations and future work

406 The model evaluation suggested that SWAT reasonably captured the hydrological and water quality behaviors in the Corn
407 Belt. However, this result could be influenced by the uncertainty of model simulations. For example, the limited number of
408 observation sites might bring uncertainties on the regional scales. The model was assessed by the best available observation
409 data, and the good agreement between the calculations and observations at 15 sites showed that the model reasonably
410 captured the changes in the water flow, TN, and TP. However, further assessment of the model is needed when more
411 observations are available.

412 The impacts of water temperature change on water quality during different El Niños were not analyzed in the study
413 because the influences of water temperature and runoff on water quality were coupled in the model. Numerical experiments
414 considering water temperature changes due to El Niños should be carried out and investigated in future studies.

415 In addition, as Chen et al. (2021) suggested that the CP-El Niño needed to be further classified into CP-I and CP-II types
416 due to the differences in sea surface temperature (SST) evolution patterns and climate impacts, the distribution of nutrients in
417 these two CP-El Niños might also differ and therefore are needed to be further studied in the future.

5 Conclusions

419 The impacts of EP- and CP-El Niños on water quality were investigated by using the SWAT model in the U.S. Corn Belt
420 region. Calibration and validation results indicated that the simulated streamflow and water quality generally agreed with
421 observations at most USGS gages. Then, the common features of the annual and seasonal loads of TN and TP for the EP-
422 and CP-El Niño events in the OTRB and UMRB were analyzed using a composite method based on the simulation results
423 during 1975–2016.

424 Annual composite results suggested that TN and TP loads decreased by 13.1% and 14.0% during EP-ENYs, respectively,
425 whereas they increased by 3.3% and 4.6% during CP-ENYs at the outlet of the OTRB, respectively. TN and TP also showed
426 a similar pattern at the outlet of the UMRB (18.5% and 19.8% reductions during EP-ENYs, and 5.7% and 4.4% increases
427 during CP-ENYs, respectively). Furthermore, more sub-basins showed negative annual anomalies of TN and TP during EP-
428 ENYs with maximum reductions up to -11.7 and -0.9 kg ha^{-1}, which were comparable to the normal year mean values (12.7
429 kg of N ha^{-1} and 1.0 kg of P ha^{-1}), respectively, whereas they showed positive anomalies during CP-ENYs.

430 Seasonal composite results confirmed that water quality anomalies showed opposite patterns during EP-ENYs and CP-
431 ENYs and the changes in the water quality matched the ENSO phases at the outlet of the OTRB. Maximum reduction or
432 increase of the nutrients during EP-ENYs or CP-ENYs, respectively, occurred in winter, the peak season of El Niño. At the
433 outlet of the UMRB (corn-growing region), TN and TP anomalies were also influenced by agriculture activities and became

Hydrology and
Earth System
Sciences
Discussions
Open Access
EGU

434 greater in spring and summer during both EP-ENYs and CP-ENYs, in consistent with the distribution of rainfall changes in

435 the basin. These results suggested that small changes in climate variables such as precipitation in the growing season could

436 have greater impacts on water quality in the UMRB during El Niño events.

437 Our analysis also found that at the outlets of UMRB and OTRB, EP-El Niño had a much greater impact on TN and TP

438 than CP-El Niño at both annual and seasonal time scales; but CP-El Niño could have comparable impacts on water quality as

439 EP-El Niño at specific watersheds or hot spots, predominantly in Iowa, Illinois, Minnesota, Wisconsin, and Indiana, which

440 contributed the greatest amounts of nutrient change to the whole basin loads.

441 Examination of the climate factors/processes on water quality change indicated that El Niño-induced precipitation and

442 temperature changes altered runoff and evaporation, and thus TN and TP in both UMRB and OTRB on annual and seasonal

443 time scales, as well as at the outlet and sub-basin scales. It is also found that nutrient levels were largely determined by

444 precipitation through runoff during both EP- and CP-ENYs, especially at the outlet, as the precipitation was a major source

445 of runoff, and nitrogen and phosphorus components were transported by runoff. At the sub-basin scale, water quality was

446 affected by the combination of precipitation and agricultural activities, especially in the UMRB during the growing season.

447 In the future when the climate continues to warm, the CP-El Niño episode is projected to occur more frequently, TN and

448 TP loads might increase in the Corn Belt region even under the same agricultural conditions, while water quality would

449 generally get better in EP-El Niño years. The findings from this study may help ensure proper decision-making for

450 watershed protection and possible ways to address anticipated water quality change associated with El Niño events.

451

452 *Data availability*. Available upon request.

453 *Author Contributions*. W.L. and P.C. designed the research; P.C. and K.H. performed the data collection and model

454 calculation; W.L. and P.C. contributed to the interpretation of the results; P.C. and W.L. wrote the manuscript.

455 *Competing Interests*. The authors declare no competing interests.

456 *Disclaimer*. Publisher's note: Copernicus Publications remains neutral with regard to jurisdictional claims in published maps

457 and institutional affiliations.

465

Hydrology and
Earth System
Sciences
Discussions

Open Access

466 **References**

467 Abbaspour, H., Saeidi-Sar, S., Afshari, H. and Abdel-Wahhab, M. A.: Tolerance of Mycorrhiza infected Pistachio (Pistacia

468   vera L.) seedling to drought stress under glasshouse conditions, J. Plant Physiol., 169(7), 704–709,

469   doi:10.1016/j.jplph.2012.01.014, 2012.

470 Afonso de Oliveira Serrão, E., Silva, M. T., Ferreira, T. R., Paiva de Ataide, L. C., Assis dos Santos, C., Meiguins de Lima,

471   A. M., de Paulo Rodrigues da Silva, V., de Assis Salviano de Sousa, F. and Cardoso Gomes, D. J.: Impacts of land use

472   and land cover changes on hydrological processes and sediment yield determined using the SWAT model, Int. J.

473   Sediment Res., doi:10.1016/j.ijsrc.2021.04.002, 2022.

474 Arnold, J. G., Srinivasan, R., Muttiah, R. S. and Williams, J. R.: Large area hydrologic modeling and assessment part I:

475   Model development, J. Am. Water Resour. Assoc., 34(1), 73–89, doi:10.1111/j.1752-1688.1998.tb05961.x, 1998.

476 Baker, N. T.: Tillage practices in the conterminous United States, 1989−2004 — Datasets aggregated by watershed, Data

477   Series 573: http://pubs.usgs.gov/ds/ds573/pdf/dataseries573final.pdf, 2011.

478 Bales, R. C., Goulden, M. L., Hunsaker, C. T., Conklin, M. H., Hartsough, P. C., O'Geen, A. T., Hopmans, J. W., and Safeeq,

479   M.: Mechanisms controlling the impact of multi-year drought on mountain hydrology, Sci. Rep., 8, 690,

480   https://doi.org/10.1038/s41598-017-19007-0, 2018.

481 Chaplot, V., Saleh, A., Jaynes, D. B. and Arnold, J.: Predicting water, sediment and NO_3-N loads under scenarios of land-use

482   and management practices in a flat watershed, Water. Air. Soil Pollut., 154(1–4), 271–293,

483   doi:10.1023/B:WATE.0000022973.60928.30, 2004.

484 Chen, M., Chang, T. H., Lee, C. T., Fang, S. W. and Yu, J. Y.: A study of climate model responses of the western Pacific

485   subtropical high to El Niño diversity, Clim. Dyn., 56(1–2), 581–595, doi:10.1007/s00382-020-05500-2, 2021.

486 Chen, P., Yuan, Y., Li, W., LeDuc, S. D., Lark, T. J., Zhang, X. and Clark, C.: Assessing the Impacts of Recent Crop

487   Expansion on Water Quality in the Missouri River Basin Using the Soil and Water Assessment Tool, J. Adv. Model.

488   Earth Syst., 13(6), doi:10.1029/2020MS002284, 2021.

489 Gassman, P. W., Reyes, M. R., Green, C. H. and Arnold, J. G.: The soil and water assessment tool: Historical development,

490   applications, and future research directions, Trans. ASABE, 50(4), 1211–1250, 2007.

491 Gershunov, A.: ENSO influence on intraseasonal extreme rainfall and temperature frequencies in the contiguous United

492   States: Implications for long-range predictability, J. Clim., 11(12), 3192–3203, doi:10.1175/1520-

493   0442(1998)011<3192:EIOIER>2.0.CO;2, 1998.

494 Johnson, M. V. V., Norfleet, M. L., Atwood, J. D., Behrman, K. D., Kiniry, J. R., Arnold, J. G., White, M. J. and Williams,

495   J.: The Conservation Effects Assessment Project (CEAP): A national scale natural resources and conservation needs

496   assessment and decision support tool, in IOP Conference Series: Earth and Environmental Science, vol. 25., 2015.

497 Kao, H. Y. and Yu, J. Y.: Contrasting Eastern-Pacific and Central-Pacific types of ENSO, J. Clim., 22(3), 615–632,

498   doi:10.1175/2008JCLI2309.1, 2009.

499 Keener, V. W., Feyereisen, G. W., Lall, U., Jones, J. W., Bosch, D. D. and Lowrance, R.: El-Niño/Southern Oscillation
500   (ENSO) influences on monthly NO3 load and concentration, stream flow and precipitation in the Little River
501   Watershed, Tifton, Georgia (GA), J. Hydrol., 381(3–4), 352–363, doi:10.1016/j.jhydrol.2009.12.008, 2010.

502 Kellner, O. and Niyogi, D.: Climate variability and the U.S. corn belt: Enso and AO episode-dependent hydroclimatic
503   feedbacks to corn production at regional and local scales, Earth Interact., 19(6), 1–32, doi:10.1175/EI-D-14-0031.1,
504   2015.

505 Kumar, K. K., Rajagopalan, B., Hoerling, M., Bates, G. and Cane, M.: Unraveling the mystery of Indian monsoon failure
506   during El Niño, Science (80-.)., 314(5796), 115–119, doi:10.1126/science.1131152, 2006.

507 Larkin, N. K. and Harrison, D. E.: On the definition of El Niño and associated seasonal average U.S. weather anomalies,
508   Geophys. Res. Lett., 32(13), 1–4, doi:10.1029/2005GL022738, 2005.

509 Lee, S. K., Mapes, B. E., Wang, C., Enfield, D. B. and Weaver, S. J.: Springtime ENSO phase evolution and its relation to
510   rainfall in the continental U.S., Geophys. Res. Lett., 41(5), 1673–1680, doi:10.1002/2013GL059137, 2014.

511 Levine, R. A. and Wilks, D. S.: Statistical Methods in the Atmospheric Sciences., 2000.

512 Li, W., Zhang, P., Ye, J., Li, L. and Baker, P. A.: Impact of two different types of El Niño events on the Amazon climate and
513   ecosystem productivity, J. Plant Ecol., 4(1–2), 91–99, doi:10.1093/jpe/rtq039, 2011.

514 Mississippi River/Gulf of Mexico Watershed Nutrient Task Force: Gulf Hypoxia: Action Plan 2008 for Reducing, Mitigating
515   and Controlling Hypoxia in the Northern Gulf of Mexico and Improving Water Quality in the Mississippi River Basin,
516   in Hypoxia in the Northern Gulf of Mexico, pp. 265–305., 2011.

517 Mo, K. C.: Interdecadal modulation of the impact of ENSO on precipitation and temperature over the United States, J. Clim.,
518   23(13), 3639–3656, doi:10.1175/2010JCLI3553.1, 2010.

519 Moriasi, D. N., Gitau, M. W., Pai, N. and Daggupati, P.: Hydrologic and water quality models: Performance measures and
520   evaluation criteria, Trans. ASABE, 58(6), 1763–1785, doi:10.13031/trans.58.10715, 2015.

521 Neitsch, S. L., Arnold, J. G., Kiniry, J. R. and Williams, J. R.: Soil and Water Assessment Tool Theoretical Documentation
522   Version 2009, Available online: http://hdl.handle.net/1969.1/128050., 2011.

523 Pagliero, L., Bouraoui, F., Willems, P. and Diels, J.: Large-Scale Hydrological Simulations Using the Soil Water Assessment
524   Tool, Protocol Development, and Application in the Danube Basin, J. Environ. Qual., 43(1), 145–154,
525   doi:10.2134/jeq2011.0359, 2014.

526 Panagopoulos, Y., Gassman, P. W., Arritt, R. W., Herzmann, D. E., Campbell, T. D., Jha, M. K., Kling, C. L., Srinivasan, R.,
527   White, M. and Arnold, J. G.: Surface water quality and cropping systems sustainability under a changing climate in the
528   Upper Mississippi River Basin, J. Soil Water Conserv., 69(6), 483–494, doi:10.2489/jswc.69.6.483, 2014.

529 Panagopoulos, Y., Gassman, P. W., Jha, M. K., Kling, C. L., Campbell, T., Srinivasan, R., White, M. and Arnold, J. G.: A
530   refined regional modeling approach for the Corn Belt - Experiences and recommendations for large-scale integrated
531   modeling, J. Hydrol., 524, 348–366, doi:10.1016/j.jhydrol.2015.02.039, 2015.

532 Panagopoulos, Y., Gassman, P. W., Kling, C. L., Cibin, R. and Chaubey, I.: Water Quality Assessment of Large-scale
533   Bioenergy Cropping Scenarios for the Upper Mississippi and Ohio-Tennessee River Basins, J. Am. Water Resour.
534   Assoc., 53(6), 1355–1367, doi:10.1111/1752-1688.12594, 2017.

535 Paul, J. H., Rose, J. B., Jiang, S. C., Zhou, X., Cochran, P., Kellogg, C., Kang, J. B., Griffin, D., Farrah, S. and Lukasik, J.:
536   Evidence for groundwater and surface marine water contamination by waste disposal wells in the Florida Keys, Water
537   Res., 31(6), 1448–1454, doi:10.1016/S0043-1354(96)00374-0, 1997.

538 Rabalais, N. N., Turner, R. E., Sen Gupta, B. K., Boesch, D. F., Chapman, P. and Murrell, M. C.: Hypoxia in the northern
539   Gulf of Mexico: Does the science support the plan to reduce, mitigate, and control hypoxia?, Estuaries and Coasts,
540   30(5), 753–772, doi:10.1007/BF02841332, 2007.

541 Ren, H. L., Lu, B., Wan, J., Tian, B., and Zhang, P.: Identification Standard for ENSO Events and Its Application to Climate
542   Monitoring and Prediction in China, J. Meteorol. Res., 32, 923–936, https://doi.org/10.1007/s13351-018-8078-6, 2018.

543 Santhi, C., Srinivasan, R., Arnold, J. G. and Williams, J. R.: A modeling approach to evaluate the impacts of water quality
544   management plans implemented in a watershed in Texas, Environ. Model. Softw., 21(8), 1141–1157,
545   doi:10.1016/j.envsoft.2005.05.013, 2006.

546 Santhi, C., Kannan, N., White, M., Di Luzio, M., Arnold, J. G., Wang, X. and Williams, J. R.: An Integrated Modeling
547   Approach for Estimating the Water Quality Benefits of Conservation Practices at the River Basin Scale, J. Environ.
548   Qual., 43(1), 177–198, doi:10.2134/jeq2011.0460, 2014.

549 Schwarz, G. E., Hoos, A. B., Alexander, R. B., and Smith, R. A.: The SPARROW Surface Water-Quality Model, U.S. Geol.
550   Surv. Tech. Methods. Sect. B, B. 6, 6-B3, 1–29, https://water.usgs.gov/nawqa/sparrow/sparrow-mod.html, 2006.

551 Sharma, S., Srivastava, P., Fang, X. and Kalin, L.: Incorporating climate variability for point-source discharge permitting in
552   a complex river system, Trans. ASABE, 55(6), 2213–2228, doi:10.13031/2013.42507, 2012.

553 Sun, G., Alstad, K., Chen, J., Chen, S., Ford, C. R., Lin, G., Liu, C., Lu, N., Mcnulty, S. G., Miao, H., Noormets, A., Vose, J.
554   M., Wilske, B., Zeppel, M., Zhang, Y., and Zhang, Z.: A general predictive model for estimating monthly ecosystem
555   evapotranspiration, 4, 245–255, https://doi.org/10.1002/eco.194, 2011.

556 Tan, W., Wei, Z., Liu, Q., Fu, Q., Chen, M., Li, B. and Li, J.: Different influences of two El Niño types on low-level
557   atmospheric circulation over the subtropical western North Pacific, J. Clim., 33(3), 825–846, doi:10.1175/JCLI-D-19-
558   0223.1, 2020.

559 Tang, T., Li, W. and Sun, G.: Impact of two different types of El Ninõ events on runoff over the conterminous United States,
560   Hydrol. Earth Syst. Sci., 20(1), 27–37, doi:10.5194/hess-20-27-2016, 2016.

561 Thomson, A. M., Brown, R. A., Rosenberg, N. J., Izaurralde, R. C., Legler, D. M. and Srinivasan, R.: Simulated impacts of
562   El Niño/Southern Oscillation on United States water resources, J. Am. Water Resour. Assoc., 39(1), 137–148,
563   doi:10.1111/j.1752-1688.2003.tb01567.x, 2003.

564 Ting, M., Seager, R., Li, C., Liu, H. and Henderson, N.: Future Summer Drying in the U.S. Corn Belt and the Role of
565   Midlatitude Storm Tracks, J. Clim., 34(22), 9043–9056, doi:10.1175/JCLI-D-20-1004.1, 2021.

566 Trenberth, K. E.: The Definition of El Niño, Bull. Am. Meteorol. Soc., 78(12), 2771–2777, doi:10.1175/1520-
567   0477(1997)078<2771:TDOENO>2.0.CO;2, 1997.

568 Twine, T. E., Kucharik, C. J. and Foley, J. A.: Effects of El Niño-Southern Oscillation on the climate, water balance, and
569   streamflow of the Mississippi River basin, J. Clim., 18(22), 4840–4861, doi:10.1175/JCLI3566.1, 2005.

570 USDA-NASS. (2016). CDL Online Website: https://nassgeodata.gmu.edu/CropScape/.

571 USDA-NASS. (2017). Census of Agriculture Online Website: https://www.nass.usda.gov/AgCensus/.

572 Vaché, K. B., Eilers, J. M. and Santelmann, M. V.: Water quality modeling of alternative agricultural scenarios in the U.S.
573   Corn Belt, J. Am. Water Resour. Assoc., 38(3), 773–787, doi:10.1111/j.1752-1688.2002.tb00996.x, 2002.

574 Wang, H. and Asefa, T.: Impact of different types of ENSO conditions on seasonal precipitation and streamflow in the
575   southeastern United States, Int. J. Climatol., 38(3), 1438–1451, doi:10.1002/joc.5257, 2018.

576 Wang, H. and Kumar, A.: Assessing the impact of ENSO on drought in the U.S. Southwest with NCEP climate model
577   simulations, J. Hydrol., 526, 30–41, https://doi.org/10.1016/j.jhydrol.2014.12.012, 2015.

578 Williams, J. R., Arnold, J. G., Kiniry, J. R., Gassman, P. W. and Green, C. H.: History of model development at Temple,
579   Texas, in Hydrological Sciences Journal, vol. 53, pp. 948–960., 2008.

580 Yeh, S. W., Kug, J. S., Dewitte, B., Kwon, M. H. and Kirtman, B. P.: El Niño in a changing climate, Nature, 461, 511–514
581   [online]   Available   from:
582   http://www.nature.com/nature/journal/v461/n7263/abs/nature08316.html%5Cnpapers2://publication/uuid/A3596821-
583   0F46-4399-A217-04ED198F5C91, 2009.

584 Yen, H., Daggupati, P., White, M. J., Srinivasan, R., Gossel, A., Wells, D., and Arnold, J. G.: Application of large-scale,
585   multi-resolution watershed modeling framework using the Hydrologic and Water Quality System (HAWQS), 8,
586   https://doi.org/10.3390/w8040164, 2016.

587 Yu, J. Y., Kao, H. Y. and Lee, T.: Subtropics-related interannual sea surface temperature variability in the central equatorial
588   pacific, J. Clim., 23(11), 2869–2884, doi:10.1175/2010JCLI3171.1, 2010.

589 Zhang, H., Wang, B., Liu, D. L., Zhang, M., Leslie, L. M. and Yu, Q.: Using an improved SWAT model to simulate
590   hydrological responses to land use change: A case study of a catchment in tropical Australia, J. Hydrol.,
591   doi:10.1016/j.jhydrol.2020.124822, 2020.

592

593